Article

Not peer-reviewed version

Synergistic Genotoxic Effects of Gamma Rays and UVB Radiation on Human Blood

Angeliki Gkikoudi , Athanasia Adamopoulou , Despoina Diamadaki , Panagiotis Matsades , Ioannis Tzakakos , Sotiria Triantopoulou , Spyridon N. Vasilopoulos , Gina Manda , Georgia I. Terzoudi , Alexandros G. Georgakilas *

Posted Date: 30 September 2025

doi: 10.20944/preprints202509.2609.v1

Keywords: gamma radiation; UVB radiation; genotoxic synergy; radiation biodosimetry; chromosomal aberrations; repair index

 doi:10.20944/preprints202509.2609.v1

Article

Synergistic Genotoxic Effects of Gamma Rays and UVB Radiation on Human Blood

Angeliki Gkikoudi [1,2], Athanasia Adamopoulou [1], Despoina Diamadaki [1], Panagiotis Matsades [1], Ioannis Tzakakos [1], Sotiria Triantopoulou [2], Spyridon N. Vasilopoulos [1], Gina Manda [3], Georgia I. Terzoudi [2] and Alexandros G. Georgakilas [1]*

[1] DNA Damage Laboratory, Physics Department, School of Applied Mathematical and Physical Sciences, tional Technical University of Athens (NTUA), Zografou Campus, 15780 Athens, Greece

[2] Health Physics, Radiobiology & Cytogenetics Laboratory, Institute of Nuclear & Radiological Sciences & Technology, Energy & Safety, National Centre for Scientific Research "Demokritos", 15341 Agia Paraskevi, Greece

[3] Radiobiology Laboratory, Victor Babeș" National Institute of Pathology, 99-101 Splaiul Independentei, 050096 Bucharest, Romania

* Correspondence: alexg@mail.ntua.gr ; AGG. Tel.: +30-210-7724453

Abstract

Exposure to ionizing and non-ionizing radiation from environmental and clinical settings can significantly threaten genomic stability, especially when combined. This ex vivo study investigates the potential combined effects of gamma radiation and ultraviolet B (UVB) light on human peripheral blood mononuclear cells (PBMCs) from healthy donors by exposing whole blood and isolated PBMCs to 1 Gy of gamma rays, 100 J/m² of UVB, or to their combination. DNA damage and repair were assessed using the γH2AX immunofluorescence assay at 1 hour and 24 hours post-irradiation. Combined exposure resulted in significantly elevated γH2AX foci formation and chromosomal aberrations relative to individual stressors, with the most pronounced effects observed in isolated PBMCs. Notably, lymphocytes from some donors failed to proliferate after UVB or co-exposure. Based on our results, a predictive biophysical model derived from dicentric yield was developed to estimate the gamma-ray equivalent dose from co-exposure, indicating a potential ~9% increase in lifetime cancer risk. These findings highlight the need to account for mixed radiation exposures in genotoxic risk assessment and radiation protection, while also supporting a protective role of the whole-blood environment.

Keywords: gamma radiation; UVB radiation; genotoxic synergy; radiation biodosimetry; chromosomal aberrations; repair index

1. Introduction

Genomic integrity is compromised by a plethora of DNA-damaging agents coming from the environmental and clinical settings, especially when cells are exposed to multiple genotoxic stresses in sequence or combination. Two such agents extensively studied and documented for their ability to induce distinct but potentially complementary forms of DNA damage are ultraviolet B (UVB) and gamma radiation. UVB radiation (280–320 nm) primarily generates bulky DNA lesions such as cyclobutane pyrimidine dimers (CPDs) and 6–4 photoproducts, which can stall replication forks and activate error-prone repair while in parallel can cause replication stress and perturb cell cycle progression, further challenging the cell's ability to maintain the mechanisms underlying DNA integrity and fidelity [1,2]. Gamma rays are high-energy photons that directly and indirectly cause DNA double-strand breaks (DSBs) and oxidatively clustered DNA lesions (OCDLs) [3]. A range of chromosomal aberrations, including dicentric chromosomes and translocations, through misrepaired DSBs are also induced by gamma rays. These aberrations are critical biomarkers of genotoxicity and

 doi:10.20944/preprints202509.2609.v1

are tightly associated with carcinogenic potential and cell death [4,5]. The sequential exposure to UVB and gamma rays results in an exacerbated burden of DSBs and increased risk of genomic instability. This combined effect is particularly important in peripheral blood mononuclear cells (PBMCs). These cells are a common model for studying genotoxicity in humans because they are accessible, sensitive to DNA damage, and play a key role in immune function [6]. We aim to explore the combined genotoxic effects of gamma radiation and UVB on isolated human PBMCs and whole blood samples by examining dicentric chromosomes and γH2AX. These are two well-known markers of DNA double-strand breaks and their repair. Our findings will help us better understand how different genotoxic mechanisms work together and what this means for human health regarding environmental and therapeutic radiation exposure. Furthermore, using our data and other existing data, we created a predictive biophysical model based on dicentric chromosome analysis. This model can accurately estimate the expected number of dicentrics after combined exposures to gamma rays and UVB. This model offers a valuable tool for assessing genotoxic risk in scenarios involving complex radiation exposure and may aid in refining biodosimetric assessments in clinical or environmental contexts.

2. Materials and Methods

2.1. Donor Recruitment and Blood Collection

Blood samples (6–7 ml) from 6 healthy donors were collected in heparin-containing vials for either *in vitro* irradiation and cell culture initiation or for lymphocyte isolation, irradiation, and fixation, depending on the assay performed. After the *in vitro* irradiation, the experimental procedures were performed according to the detailed protocols described in the next paragraphs. Written informed consent was obtained, as the project involves the use of human genetic material and biological samples, according to ethics protocol number 21/12/2023-17 (Date: 21/02/2023) NCSR 'Demokritos' bioethics committee. For additional information, see Section S1 in the Supplementary File.

2.2. Preparation of samples and irradiation protocol

Peripheral blood (1 ml) was diluted (1:1) in RPMI 1640 cell culture medium and placed in 3.5 cm petri dishes for irradiation. After irradiation, samples were held for 20 minutes and 24 hours at 37°C. PBMCs were then isolated using an equal volume of Lymphosep Separating Media (L0560, Biowest, Nuaillé, France), following standard procedures [7].When directly irradiating PBMCs, isolation was performed before irradiation. Whole blood and isolated lymphocyte cultures were irradiated using a gamma radiation source of Cobalt-60 (Co-60) located at the National Centre for Scientific Research "Demokritos" in Athens, Greece. The Co-60 source delivers a dose rate of 0.10 Gy/min, ensuring consistent and precise irradiation exposure of samples. Before irradiation, the dose rate was verified using a calibrated dosimeter to confirm the accuracy of the applied dose. After approximately 15 min, samples kept at room temperature (RT) were exposed to UVB by using the UV Bench Lamp Model XX-15M, with a power output of 15 watts and a peak emission at 302 nm. The lamp was calibrated before each experiment to ensure accurate UVB exposure. Samples were positioned at a fixed distance from the lamp to achieve reproducible irradiation. The exposure times and distances were carefully controlled to deliver the desired UVB dose, and all procedures were conducted under standardized laboratory conditions to ensure reproducibility. For additional information, see Section S2 in the Supplementary File.

2.3. Dicentric Chromosome Assay

For dicentric chromosome analysis, whole blood and isolated PBMCs were cultured in RPMI 1640 medium containing 10% fetal bovine serum, 1% glutamine, and antibiotics [penicillin: 10,000 U/ml; streptomycin: 10,000 μg/ml (Sigma-Aldrich)]. Phytohaemagglutinin (PHA) was dissolved in

 doi:10.20944/preprints202509.2609.v1

PBS at a concentration of 0.24 mg/ml. Cultures were incubated at 37°C in a humidified incubator in an atmosphere of 5% CO_2 and 95% air for 50 h. Colcemid solution was added 3 h before cell harvest, and cells were collected by centrifugation, treated in 75 mM KCl for 10 min, fixed in methanol: glacial acetic acid 3:1 (v/v) and processed for cytogenetic analysis. Giemsa staining was achieved by immersing slides in 2% Giemsa solution for 10 min, then washing with distilled water and air-drying. Slides were covered with coverslips and analyzed using a microscope (Axioplan 2, Carl Zeiss Microscopy GmbH, Hamburg, Germany). The chromosome aberration analysis was greatly facilitated by the dedicated IKAROS software for the semi-automated image analysis (MetaSystems, Germany). The number of metaphases analyzed for each experimental time point was 500.

2.4.γ. H2AX Foci Analysis for Estimation of the DSBs and Repair

H2AX phosphorylation detection was performed by using a modification of the protocol of Tremi et al. [8]. Briefly, cell suspensions (PBMCs) were centrifuged on microscope slides using a Cytospin ROTANTA 460/460R centrifuge (Hettich, Tuttlingen, Germany), fixed for 15 min at RT with 3% paraformaldehyde (F8775, Sigma-Aldrich, Darmstadt, Germany) and 2% sucrose (A2211, Applichem GmbH, Darmstadt, Germany) in phosphate-buffered saline (PBS, 18912-014, Gibco, Grand Island, NY, USA), and then triple-washed with PBS. Cells were thereafter permeabilized for 10 min with 0.5% Triton X-100 (X100, Merck, Saint Louis, MO, USA) in 100 mM Tris-HCL pH 7.4 (A4263, Applichem GmbH, Darmstadt, Germany) and 50 mM EDTA pH 8 (A4982, AppliChem GmbH, Darmstadt, Germany) in distilled water, washed again three times with PBS, and blocked overnight at 2-8 °C with 0.5% bovine serum albumin (BSA, A7906, Sigma-Aldrich, Darmstadt, Germany) and 0.2% gelatin from cold water fish (G7041, Sigma-Aldrich, Darmstadt, Germany) in PBS. Cells were incubated for 90 min at RT with an antibody against histone H2AX (phospho S139) (NB100-384, Novus Biologicals, Abingdon, UK) in 0.5% BSA and 0.2% gelatin in PBS, and then were washed three times with PBS. A 90 min incubation at RT with goat anti-rabbit IgG H&L cross-absorbed secondary antibody labeled with Rhodamine Red-X (R-6394, Thermo Fisher Scientific, Waltham, MA, USA) in 0.5% BSA and 0.2% gelatin in PBS followed. After 3x washing with PBS, DNA was counter-stained with ProLong Gold Antifade Reagent with 4'6-diamidino-2-phenylindole (DAPI) (8961, Cell Signaling Technology Inc, Danvers, MA, USA), and cells were shielded with 22x22 mm coverslips, avoiding air bubble trapping. Two independent experiments were conducted for each donor. Microscope slides were analyzed using a Zeiss Axioskop-2 fluorescence microscope with ISIS software. More than 100 cells/slide were analyzed with the JCountPro and JQuantPlus image processing software (courtesy of Dr. Pavel Lobachevsky group, Peter McCallum Institute, Australia) [9].

3. Results

3.1. DNA Damage measurement

The evaluation of DNA damage responses in PBMCs following exposure to ionizing and non-ionizing radiation was performed by quantifying γH2AX foci per nucleus in both whole blood and isolated PBMCs from three different donors. Samples were exposed to 1 Gy gamma radiation or 100 J/m² UVB, and to a combination of both stressors (gamma radiation followed by UVB 20 minutes later). Irradiated samples and sham-irradiated controls were analyzed at 1 h and 24 h post-exposure. Elevated levels of γH2AX foci were detected in whole blood samples (Figures 1a–c) at 1 h post-irradiation compared to controls, across all donors. The greatest increase was observed following 1 Gy exposure, with a moderate but consistent rise in foci after combined treatment. By 24 h, γH2AX foci generally declined toward baseline, although residual damage remained notably higher in the combined treatment group compared to single stressor exposures. A similar trend was observed in isolated PBMCs (Figures 1d–f), with robust γH2AX induction at 1 h following gamma irradiation (1 Gy) and combined exposures to gamma rays and UVB. Meanwhile, the combined treatment group consistently exhibited the highest γH2AX foci at both time points, suggesting additive or synergistic

 doi:10.20944/preprints202509.2609.v1

effects of sequential gamma and UVB exposure. UVB alone induced modest γH2AX formation, especially when compared to gamma radiation. When averaged across all donors (Figure 1g), the data confirmed higher γH2AX foci induction in isolated PBMCs than in PBMCs irradiated in whole blood, particularly in response to combined exposure. Furthermore, while γH2AX foci levels declined by 24 h post-irradiation, they remained elevated relative to the baseline, especially in samples subjected to combined stressors. A representative dose–effect curve obtained from the first donor's isolated PBMCs, illustrating the linear relationship between the absorbed gamma dose and γH2AX foci formation, is provided in Supplementary Figure S3.

Overall, results demonstrate that a combined exposure to gamma radiation and UVB induces increased levels of DNA damage compared to each single stressor, with isolated PBMCs displaying a more pronounced response than whole blood samples. The time-dependent decrease in γH2AX foci suggests ongoing DNA repair, although residual damage remains evident at 24 h post-exposure.

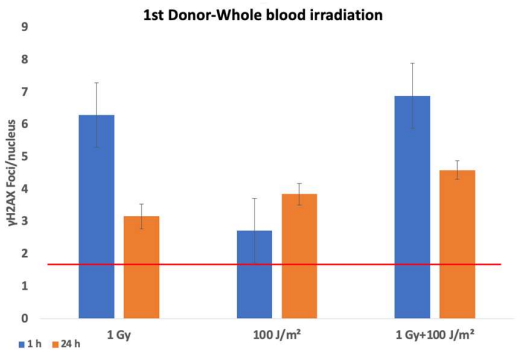

(a)

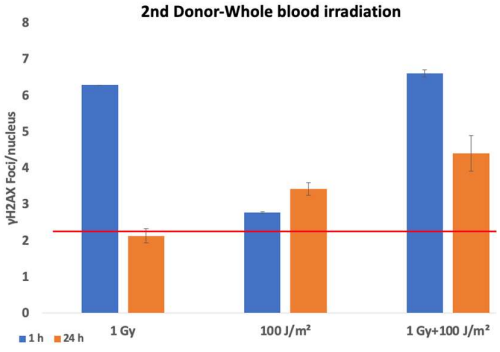

(b)

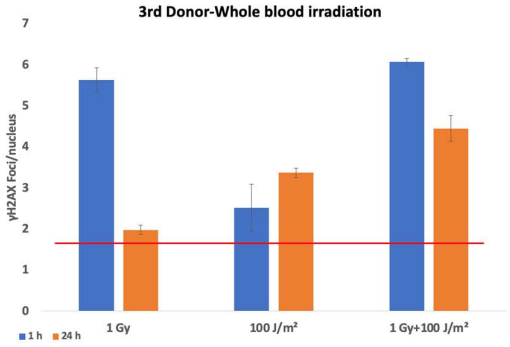

(c)

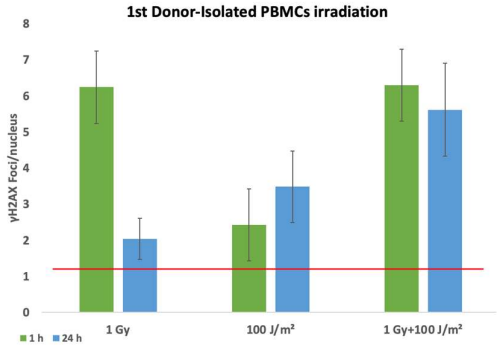

(d)

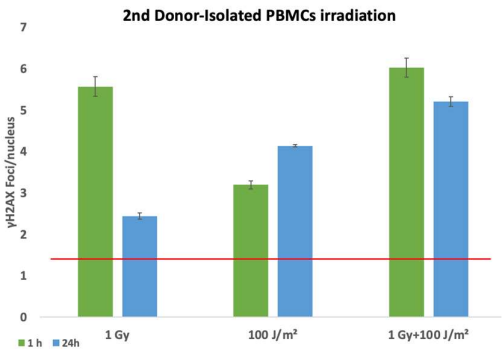

(e)

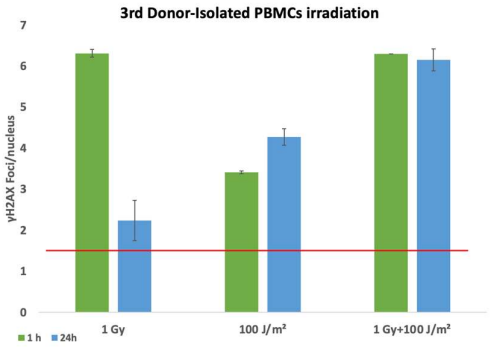

(f)

 doi:10.20944/preprints202509.2609.v1

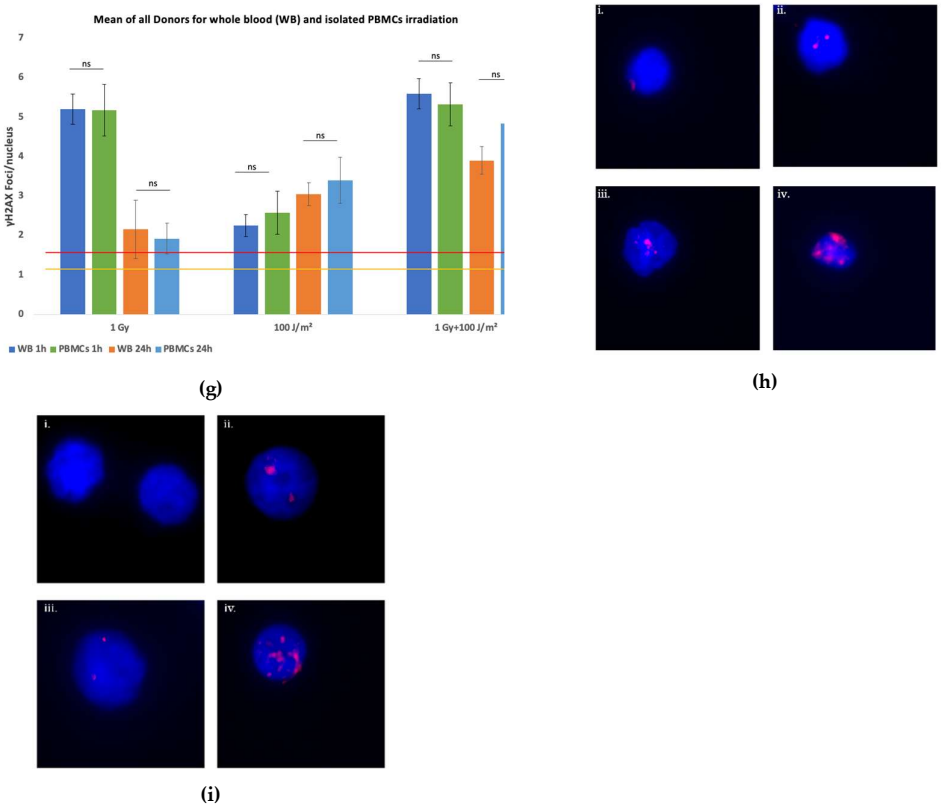

Figure 1. γH2AX staining in PBMCs following co-exposure to gamma rays and UVB. Results are presented as mean effect (value) ± standard deviation (SD) from 2 independent experiments. The red line designates the mean value in control samples. (a) γH2AX foci per nucleus in 1st donor PBMCs at 1 h and 24 h after exposure of whole blood to 1 Gy gamma rays or 100 J/m² UVB as single stressors, or to combined challenges (gamma rays first, and UVB 20 min thereafter) (the standard deviation for control sample is 0.02 foci/nucleus); (b) γH2AX foci per nucleus in 2nd donor PBMCs at 1 h and 24 h after exposure of whole blood to 1 Gy gamma rays or 100 J/m² UVB as single stressors, or to combined challenges (gamma rays first, and UVB 20 min thereafter) (the standard deviation for control sample is 0.13 foci/nucleus); (c) γH2AX foci per nucleus in 3rd donor PBMCs at 1 h and 24 h after exposure of whole blood to 1 Gy gamma rays or 100 J/m² UVB as single stressors, or to combined challenges (gamma rays first, and UVB 20 min thereafter) (the standard deviation for control sample is 0.24 foci/nucleus) (d) γH2AX foci per nucleus in 1st donor PBMCs at 1 h and 24 h after exposure of isolated PBMCs to 1 Gy gamma rays or 100 J/m² UVB as single stressors, or to combined challenges (gamma rays first, and UVB 20 min thereafter) (the standard deviation for control sample is 0.26 foci/nucleus) (e) γH2AX foci per nucleus in 2nd donor PBMCs at 1 h and 24 h after exposure of isolated PBMCs to 1 Gy gamma rays or 100 J/m² UVB as single stressors, or to combined challenges (gamma rays first, and UVB 20 min thereafter) (the standard deviation for control sample is 0.18 foci/nucleus); (f) γH2AX foci per nucleus in 3rd donor PBMCs at 1 h and 24 h after exposure of isolated PBMCs to 1 Gy gamma rays or 100 J/m² UVB as single stressors, or to combined challenges (gamma rays first, and UVB 20 min thereafter) (the standard deviation for control sample is 0.11 foci/nucleus); (g) Mean of all cultures for whole blood and isolated PBMCs irradiation (the standard deviation for control sample for whole blood is 0.25 foci/nucleus and represented with the red horizontal line and for isolated PBMCs is 0.29 foci/nucleus and represented with the yellow horizontal line). (h) Fluorescence images (γH2AX) of PBMCs following co-exposure of whole blood to gamma rays and UVB: (i) unirradiated, (ii) exposed to 100 J/m² UVB, (iii) exposed to 1 Gy gamma rays and (iv) co-exposed to 1 Gy gamma rays and 100 J/m² UVB all 24 h post-exposure (blue signal: cell nucleus, red signal: γH2AX foci); (i) Fluorescence images of PBMCs following co-exposure of isolated PBMCs to gamma rays and UVB: (i) unirradiated, (ii) exposed to 100 J/m² UVB, (iii) exposed to 1 Gy gamma rays and (iv) co-exposed to 1 Gy gamma rays and 100 J/m² UVB all 24 h post-exposure (blue signal: cell nucleus, red signal: γH2AX foci).

 doi:10.20944/preprints202509.2609.v1

The assessment of DNA repair efficiency under all exposure conditions, both in whole blood and isolated PBMCs, was estimated with the calculation of the repair index for each donor (Table 1) by subtracting the number of γH2AX foci at 24 h (F_{24}) from the number of γH2AX foci at 1 h (F_1) and dividing to the number of γH2AX foci at 1 h ie. Repair index (RI)= $(F_1 - F_{24})/F_1$.

This metric provides a relative measure of DNA repair capacity. A lower repair index suggests limited repair or persistent damage ($F_{24}\uparrow$), while a higher repair index indicates a reduction in γH2AX foci, reflecting efficient DNA repair ($F_{24}\downarrow$). This calculation enables a direct comparison of repair dynamics between whole blood and isolated PBMCs. In whole blood samples, all three donors exhibited a decrease in γH2AX foci by 24 h as compared to the 1 h time point, with the repair index indicating more effective repair after 1 Gy exposure compared to combined treatment or UVB alone. The 3rd donor showed the lowest repair index for the co-exposure condition, suggesting slower repair or persistent damage, whereas the 2nd donor displayed a relatively better repair capacity overall. In isolated PBMCs, the repair index was generally lower than in whole blood in the co-exposure condition, indicating delayed or incomplete repair and greater susceptibility to persistent DNA damage.

Table 1. Repair index (RI) for each donor under all exposure conditions, both in whole blood (WB) and isolated PBMCs.

Donors	RI-1 Gy gamma rays	RI-1 Gy gamma rays+100 J/m²
1st	WB: 0.45 PBMCs: 0.67	WB: 0.30 PBMCs: 0.11
2nd	WB: 0.66 PBMCs: 0.56	WB: 0.33 PBMCs: 0.14
3rd	WB: 0.65 PBMCs: 0.65	WB: 0.27 PBMCs: 0.02

3.2. Synergy evaluation – the Bliss Independence Model

To better understand and evaluate the nature (additive or synergistic) of the combined action of gamma and UVB radiation and examine whether its induced biological effects are synergistic or just additive in terms of DNA damage, the Bliss Independence Model was used in both whole blood and isolated PBMCs, based on the detected foci counts. The Bliss Independence Model, built on the probability theory of independent events, is one of the most widely used synergy metrics. This model is mainly used to evaluate drug combination efficacy through the calculation of the expected combined effects of two drugs, and subsequent comparison with the corresponding observed effects [10,11].

All calculations and comparisons, the single activities of agents, as well as the observed effect of their combination, should be expressed as a probability between 0 and 1, meaning that all values used by the Bliss Independence Model should be normalized to a 0-1 scale before any calculation (https://gdsc-combinations.depmap05082023.sanger.ac.uk/documentation, assessed 20/09/2025). Derived from the complete additivity of the probability theory, where the assumption that the agents act independently means that the combined effect is equal to the product of their individual effects, according to the formula: $(1 - E_{AB\_exp}) = (1 - E_A) \cdot (1 - E_B)$. By solving this, we take the Bliss Independence Model formula:

$$E_{AB\_exp} = E_A + E_B - E_A \cdot E_B \qquad [3.2.1]$$

The method compares the observed effect ($E_{AB_{obs}}$) induced by the combination of agents A and B with the expected corresponding effect (E_{AB_exp}), which was obtained based on the assumption that there is no agent-agent interaction effect. Typically, the combination effect is declared synergistic if E_{AB_obs} is higher than E_{AB_exp} [11]. For a more direct comparison, the Bliss excess is usually

 doi:10.20944/preprints202509.2609.v1

calculated as $\Delta = E_{AB\_obs} - E_{AB\_exp}$ and the effect induced by the combination of agents A and B is characterized according to the value of Δ, as summarized below:

$$\Delta \begin{cases} > 0, & \text{synergistic} \\ = 0, & \text{additive} \\ < 0, & \text{antagonistic} \end{cases} \qquad [3.2.2]$$

In this study, we evaluated the combined DNA-damaging effects of gamma and UVB radiation using the Bliss Independence Model. Analysis was performed on γH2AX immunofluorescence data (foci counts) at 24 h post-irradiation in both isolated PBMCs and whole blood. We focused on the 24 h time point, as synergy—if present—is expected to emerge later rather than at 1 h. Experiments were conducted in three donors, with two replicates per donor (A and B). Mean values of foci counts were normalized to a 0–1 scale using the formula:

$$E_x^{norm} = \frac{(Foci\ count)_x - control}{max\ observed - control} \qquad [3.2.3]$$

here 0 = baseline (control) and 1 = maximal effect (highest foci count in co-exposure). In all cases, maximum damage occurred in the combined gamma and UVB exposure.

Under the Bliss model, gamma and UVB are considered independent, each inducing normalized effects E_γ and E_{UVB}. The expected combined effect is:

$$E_{gamma-UVB}^{exp} = E_{gamma} + E_{UVB} - E_{gamma} \cdot E_{UVB}$$

Having calculated the expected biological effect from the Bliss model (Table 2), to evaluate the combined action of gamma and UVB and characterize it as synergistic or just additive, Bliss excess values have been estimated based on the equation:

$$\Delta = E_{gamma-UVB}^{obs} - E_{gamma-UVB}^{exp} \qquad [3.2.5]$$

Observed, expected, and excess values for all donors and conditions are summarized in Table 2.

Table 2. Observed (obs) and expected (exp) biological effect induced by the combination of gamma and UVB radiation and Bliss excess values (Δ) for each donor at 24 h post-irradiation, both in whole blood (WB) and in isolated PBMCs, calculated using the Bliss Independence Model.

	Whole Blood			**Isolated PBMCs**		
	1st donor	2nd donor	3rd donor	1st donor	2nd donor	3rd donor
$E_{gamma-UVB}^{obs}$	1	1	1	1	1	1
$E_{gamma-UVB}^{exp}$	0.854744719	0.569017759	0.622986037	0.631372378	0.661847612	0.796975071
Bliss excess (Δ)	0.145255281	0.430982241	0.377013963	0.368627622	0.338152388	0.203024929

As shown from the table above (Table 2), for each donor and both in whole blood and in isolated PBMCs, all the values for the Bliss excess (Δ) were higher than zero. In accordance with the Bliss Independence Model, this indicates that gamma and UVB radiation, when combined, induce a biological effect that exceeds the effect of each radiation type alone, suggesting a potentially synergistic, rather than merely additive, interaction in terms of induced DNA damage.

To verify that the interaction of gamma and UVB is truly synergistic, we proceeded with a one-sample t-test. This approach allows for the comparison of the mean Bliss excess values ($\bar{\Delta}$) against zero, for investigating whether the observed synergy (in each donor in whole blood and in isolated PBMCs) was statistically significant. It should be noted that in the one-sample t-test the comparison of the mean Bliss excess was conducted against zero, since zero corresponds to the null hypothesis-namely, the absence of synergy.

The one-sample t-test revealed that the mean Bliss excess $\bar{\Delta}$ was significantly higher than zero in both experimental conditions (irradiated whole blood and isolated PBMCs), validating the synergistic action of gamma and UVB radiation in terms of induced DNA damage. More precisely,

 doi:10.20944/preprints202509.2609.v1

in whole blood, the mean $\bar{\Delta}$ value obtained from the three independent experiments was 0.32 ± 0.15, with the t-test revealing that this mean was significantly higher than zero ($t(2) = 3.63, p - value = 0.034$) Similarly, in isolated PBMCs the corresponding $\bar{\Delta}$, derived again from three independent experiments, was 0.30 ± 0.09, with the t-test confirming a statistically significant difference from zero ($t(2) = 5.96, p - value = 0.014$, further supporting the presence of synergy in the combined action of gamma and UVB regarding radiation-induced DNA damage.

The aforementioned analysis and the results obtained from the Bliss Independence Model contribute to a growing body of evidence suggesting that the combined action of gamma and UVB radiation can produce a greater biological effect than that induced by their corresponding additive action. These findings indicate a synergistic rather than additive interaction between gamma and UVB, based on the statistically higher DNA damage induced by the combination of these two types of radiation, as observed in both whole blood and isolated PBMCs experiments.

3.3. Genomic instability-Chromosomal aberrations assay

Chromosomal instability was evaluated by quantifying dicentric chromosomes (dic) and acentric fragments (ace) in lymphocytes from three donors following exposure to 1 Gy gamma rays, 100 J/m² UVB, or a combination of both (gamma rays followed by UVB). The data are presented as mean aberrations per cell ± SD from two independent experiments. In all three investigated donors (Figures 2a–f), exposure to 1 Gy gamma rays induced a notable increase in both dicentrics and acentric fragments compared to control values. UVB exposure alone resulted in minimal chromosomal damage, whereas combined treatment (1 Gy + 100 J/m²) consistently led to the highest levels of aberrations. This additive effect was evident in all donors, with the third donor (Figures 2e–f) exhibiting a similar pattern to donors one and two. Specifically, dicentric frequency more than doubled under co-exposure conditions relative to 1 Gy alone, and a substantial increase in acentric fragments was also observed. Importantly, representative metaphase spreads from lymphocytes subjected to combined exposure revealed complex chromosomal damage, including the presence of both chromosomal exchanges and acentric fragments (Figure 2g), reinforcing the enhanced genotoxic effect of combined radiation fields.

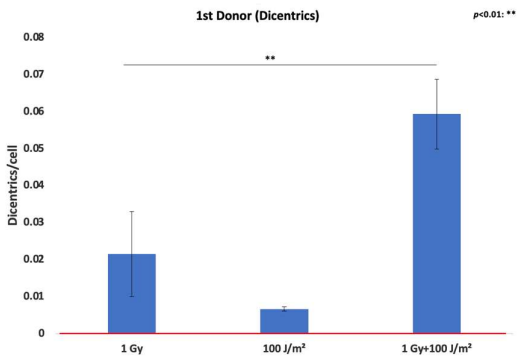

(a)

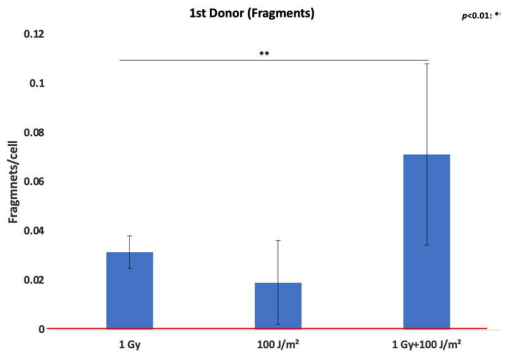

(b)

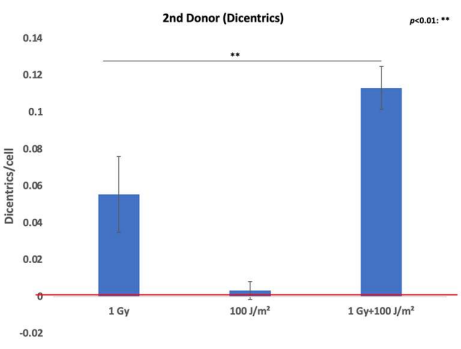

(c)

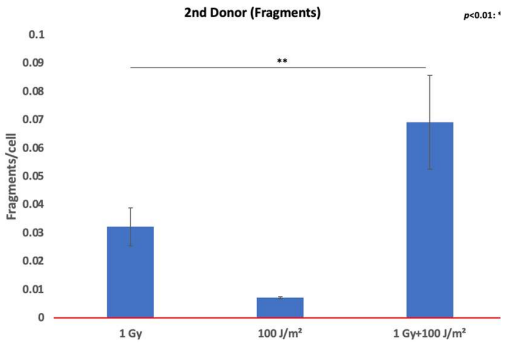

(d)

 doi:10.20944/preprints202509.2609.v1

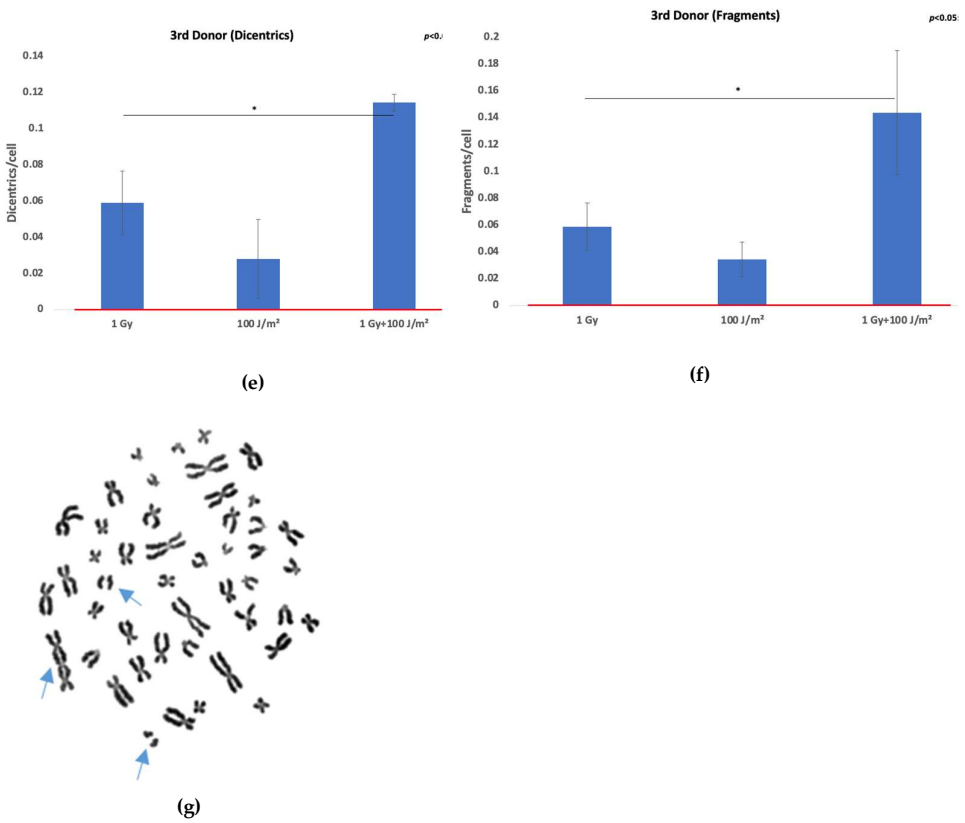

Figure 2. Chromosomal aberrations in lymphocytes. Results are presented as mean effect (value) ± SD for 2 independent experiments. The red line designates the mean value in control samples. (a) Dicentrics frequencies in PBMCs induced by exposure of whole blood to 1 Gy gamma rays or 100 J/m² UVB as single stressors, or to combined challenges for the 1st donor (the standard deviation for control sample is 0.01 dic/cell); (b) Acentric fragments frequencies in PBMCs induced by exposure of whole blood to 1 Gy gamma rays or 100 J/m² UVB as single stressors, or to combined challenges for the 1st donor (the standard deviation for control sample is 0.007 ace/cell); (c) Dicentrics frequencies in PBMCs induced by exposure of whole blood to 1 Gy gamma rays or 100 J/m² UVB as single stressors, or to combined challenges for the 2nd donor (the standard deviation for control sample is 0.02 dic/cell); (d) Acentric fragments frequencies in PBMCs induced by exposure of whole blood to 1 Gy gamma rays or 100 J/m² UVB as single stressors, or to combined challenges for the 2nd donor the standard deviation for control sample is 0.007 ace/cell); (e) Dicentrics frequencies in PBMCs induced by exposure of whole blood to 1 Gy gamma rays or 100 J/m² UVB as single stressors, or to combined challenges for the 3rd donor (the standard deviation for control sample is 0.02 ace/cell); (f) Acentric fragments frequencies in PBMCs induced by exposure of whole blood to 1 Gy gamma rays or 100J/m² UVB as single stressors, or to combined challenges for the 3rd donor (the standard deviation for control sample is 0.02 ace/cell).

Chromosomal aberration analysis was also attempted in isolated lymphocytes from the third donor for the same exposure conditions. Isolated lymphocytes failed to yield analyzable metaphase spreads following UVB or combined treatment. Mitotic index measurements revealed that these conditions led to a marked reduction in proliferating cells, indicating a strong cytostatic or cytotoxic response ($MI_{control}$=0.0068, MI_{1Gy}=0.0056, $MI_{100J/m2}$=0 and $MI_{1Gy+100J/m2}$). To investigate whether this proliferative inhibition could be overcome, additional experiments were performed using a higher gamma rays dose of 2 Gy and a lower UVB fluence of 25 J/m². These irradiation conditions were applied to both whole blood and isolated lymphocytes. Results are shown in Figure 3, and further support the differential responses and DNA damage outcomes between whole blood and isolated lymphocyte preparations (χ^2 test, $p<0.05$ in co-exposure condition).

 doi:10.20944/preprints202509.2609.v1

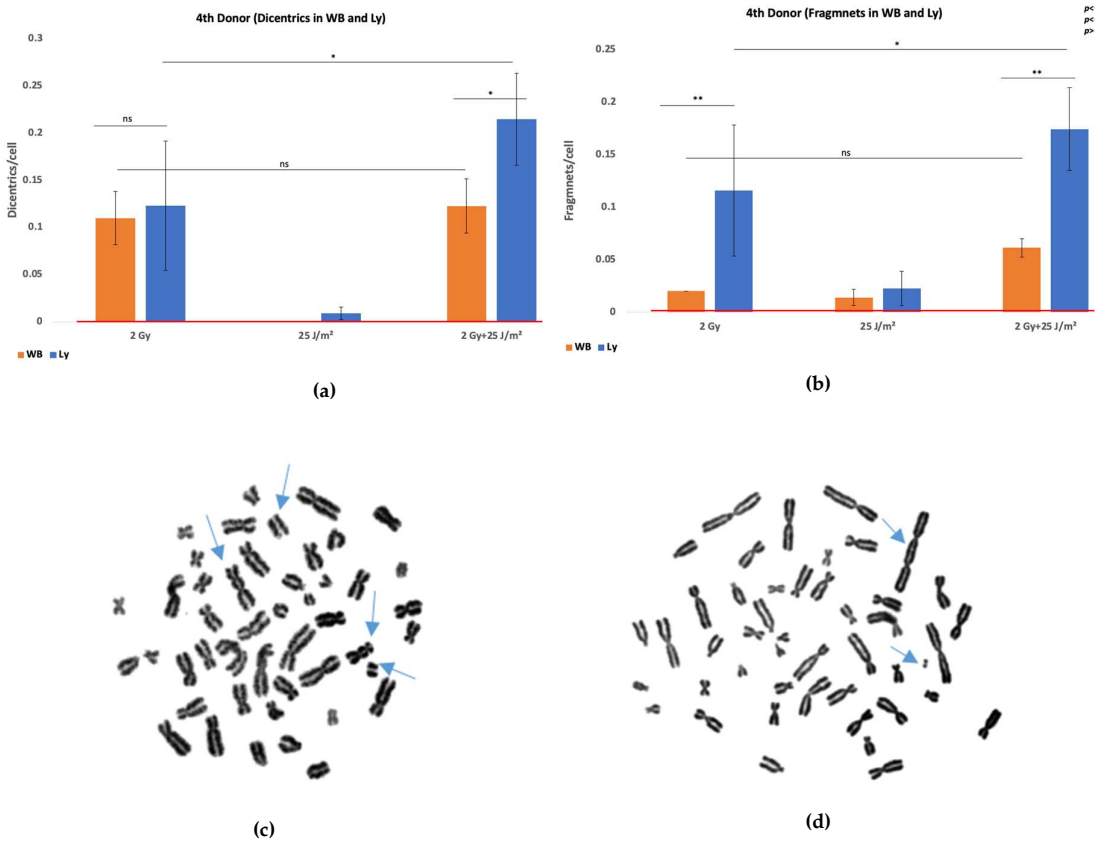

Figure 3. Chromosomal aberrations in lymphocytes of 4th donor. (a) Dicentrics frequencies in lymphocytes induced by exposure of whole blood and isolated PBMCs to 2 Gy gamma rays or 25 J/m² UVB as single stressors, or to combined challenges (the standard deviations for control sample for whole blood and isolated lymphocytes are both 0 dic/cell).; (b) Acentric fragments frequencies in PBMCs induced by exposure of whole blood and isolated lymphocytes to 2 Gy gamma rays or 25 J/m² UVB as single stressors, or to combined challenges (the standard deviations for control sample for whole blood and isolated lymphocytes are both 0.04 ace/cell); (c) Metaphase spread of isolated lymphocytes exposed to 2 Gy gamma rays and 25 J/m² UVB with two dicentric chromosomes and two acentric fragments and (d) Metaphase spread of PBMCs whole blood exposure to 2 Gy gamma rays and 25 J/m² UVB with a dicentric chromosome and an acentric fragment.

3.4. Extension of the Linear-Quadratic Model to Predict Dicentric Chromosome Yield Following Co-Exposure of Whole Blood or Isolated PBMCs to Gamma and UVB Radiation

The elevated dicentric frequency cannot be explained by additive effects alone and aligns with observations of synergistic interactions between UVB and ionizing radiation exposures. To better capture this phenomenon, we extended the traditional linear-quadratic model by incorporating an exponential synergy term, as supported by our mechanistic and empirical findings. The standard LQ model, described by the expression $Y = \alpha D + \beta D^2$, where Y is the yield of dicentrics per cell and D is the dose of ionizing radiation, captures the linear contribution (α) of single radiation-induced events and the quadratic component (β) associated with interactions between two DNA damage events [12]. To accommodate non-ionizing UVB radiation, an additional linear term γD_{UVB} was introduced, where γ represents the independent contribution of UVB to dicentric formation—typically small or negligible under most exposure conditions.

Crucially, a synergy term $\delta D_{DUVB} \cdot e^{(-\Delta t/20)}$ was included to model the interaction between gamma rays and UVB, where δ is the synergy coefficient, D and D_{UVB} are the respective doses, and Δt is the time interval between exposures, reflecting temporal effects on biological repair processes. This term describes the enhanced DNA damage observed when co-exposure overwhelms repair mechanisms,

 doi:10.20944/preprints202509.2609.v1

resulting in a non-linear increase in dicentrics. Importantly, w_{order}, order index, is a dimensionless parameter that encodes the sequence of exposure: it equals 1 when gamma radiation follows UVB (a configuration known to produce stronger synergistic effects due to UVB-induced replication stress or repair interference) and is set to 0.1-0.2 when the order is reversed, while being set to 0.5 for simultaneous exposures [13]. This index ensures that the model reflects empirical observations where the timing of radiation delivery significantly influences dicentric yield. A residual error term ε is incorporated to account for biological variability and measurement uncertainty. The proposed extension of the linear-quadratic model is given by the equation:

$$\Upsilon_{Dic/cell} = \alpha \cdot D + \beta \cdot D^2 + \gamma \cdot D_{UVB} + \delta \cdot D \cdot_{UVB} \cdot e^{(-\Delta t/20) \cdot} w_{order} + \varepsilon \qquad [\ 3.4.1\ ]$$

Using parameter values derived from literature and our experimental setup ($\alpha = 0.05$, $\beta = 0.01$, $\delta = 0.007$, $w_{order} = 0.1$, $\Delta t = 15$, $D = 1$ Gy, $D_{UVB} = 100$ J/m², $\varepsilon = 0.01$), the model predicted a dicentric yield of 0.103 dicentrics/cell under co-exposure conditions. For additional information please see the Section 4 of Supplementary File.

Compared to our results, the model accurately captured the observed yields for donors 2 and 3, with deviations of less than 10%, confirming its validity in simulating co-exposure-induced genomic instability. For donor 1, the observed yield was substantially lower than predicted, suggesting individual variability in radiosensitivity or DNA repair capacity. These results underscore the predictive utility of the extended LQ model, particularly in mixed-radiation contexts, and highlight the importance of introducing exposure timing and sequence when modeling complex biological responses. To further evaluate the predictive accuracy of our extended linear-quadratic model, we applied it to WB data from a fourth donor exposed to 2 Gy gamma radiation or 25 J/m² UVB, and their combination. The model predicted dicentric yields of 0.150, 0.010, and 0.167 dicentrics/cell for the respective conditions. Having obtained 0.11 for 2 Gy only, 0.01 for UVB only, and 0.12 for the combined exposure, the model performed well for UVB and reasonably well for gamma radiation, but in the co-exposure condition did slightly overpredict the dicentric yield by about 0.047 dicentrics/cell.

This probably outlines the biological 'buffering' and protective capacity of whole blood and the potential moderating effect it has over the synergism in relation to isolated lymphocytes, as explained in greater detail in the following section. Despite this limitation, the model successfully captures both the direction and magnitude of the observed synergy, supporting its applicability in mixed-radiation biodosimetry and highlighting the importance of sample context (whole blood vs. isolated lymphocytes) in interpreting cytogenetic outcomes.

4. Discussion

No significant differences were revealed through γH2AX foci analysis of DNA damage between isolated PBMCs and whole blood across all tested conditions (1 Gy gamma rays, 100 J/m² UVB, and their combination) at both 1 h and 24 h post-irradiation (t-test, $p>0.05$ in all condtitions). This suggests that the immediate induction and short-term repair kinetics of DSBs were comparable between the two systems. However, a divergent pattern emerged when chromosomal damage was evaluated via the dicentric assay. In the 1 Gy gamma rays and 100 J/m² UVB co-exposure group, isolated lymphocytes exhibited significant cell death, precluding dicentric scoring, whereas lymphocytes in whole blood survived and displayed dicentric yields consistent with synergistic damage. These findings emphasize that while γH2AX foci reflect early and direct DSB formation, the dicentric assay is more sensitive to cumulative biological effects, including survival and repair dynamics. Using both γH2AX foci analysis and dicentric chromosome assays in mixed radiation exposures gives a comprehensive assessment of DNA damage and genomic instability. Together, these biomarkers form a synergistic paradigm for understanding radiation-induced genomic instability, capturing both acute DNA damage signaling and its downstream cytogenetic consequences. Crucially, their combined use emphasizes the need for multi-endpoint methods for

 doi:10.20944/preprints202509.2609.v1

precise biodosimetry and risk evaluation in situations where ionizing and non-ionizing radiation exposure occurs sequentially or simultaneously (Figure 3). The comparatively small number of blood samples examined in this study is a limitation that might restrict how broadly the results can be applied; nonetheless, the primary goal was to outline the methodology and show how the aforementioned biomarkers could be used to evaluate DNA damage after combined exposures.

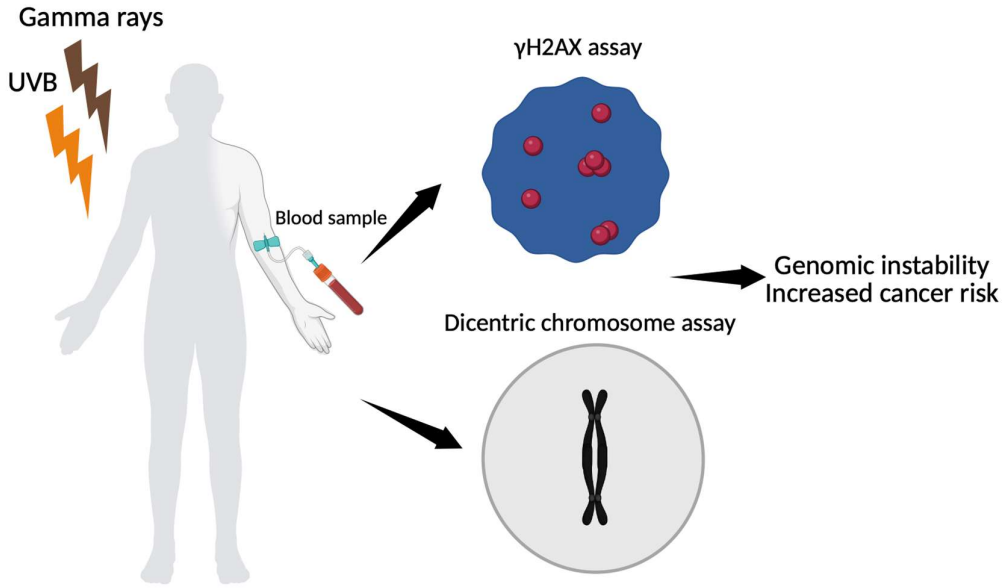

Figure 3. Schematic representation of biomarker-based assessment of genomic instability following gamma ray and UVB exposure. Peripheral blood mononuclear cells are analyzed using γH2AX immunofluorescence assay to quantify DNA double-strand breaks and dicentric chromosome assay to measure chromosomal aberrations. Both endpoints contribute to the evaluation of genomic instability after co-exposure (The figure was created using Biorender available at https://app.biorender.com (accessed on 10 July 2025).

The estimated repair index further supports the differences in long-term cellular outcomes, as across all donors and exposure types, isolated PBMCs consistently showed lower values than whole blood, particularly in co-exposure conditions, indicating a reduced ability to resolve DNA damage over time. Furthermore, exposure to a sub-toxic dose of 2 Gy gamma rays and 25 J/m² UVB showed a synergistic increase in dicentrics in the remaining viable isolated lymphocytes, with no effect in whole blood, suggesting that plasma-mediated protective mechanisms blunted the synergy. The observed discrepancy between isolated lymphocytes and whole blood may also reflect the intrinsic protective and reparative properties of the blood matrix.

Our findings align with growing evidence that blood, particularly its plasma components, plays a significant protective role against UVB-induced oxidative damage. Plasma contains a variety of endogenous antioxidants—including uric acid, vitamin C, and thiol-containing proteins—which scavenge reactive oxygen species (ROS) generated during UVB exposure [14]. Human serum albumin (HSA), via its Cys34 thiol, contributes roughly 40–70% to this capacity, and, in some contexts, the thiol itself accounts for up to 80% of albumin's radical-scavenging activity [15-18]. Uric acid (urate) provides over half of the antioxidant potential in plasma [19], acting as a scavenger of ROS such as peroxyl, and hydroxyl radicals [20]. In addition, erythrocytes contain robust enzymatic antioxidants—catalase, glutathione peroxidase, and superoxide dismutase—that constitute a first-line defense against ROS in the blood, rapidly detoxifying hydrogen peroxide and superoxide anions [21,22]. This multienzyme system is essential for protecting hemoglobin and maintaining redox

 doi:10.20944/preprints202509.2609.v1

balance in circulating blood. By lowering extracellular ROS levels, erythrocytes likely mitigate ROS-mediated secondary oxidative DNA damage in co-circulating lymphocytes. In parallel, the presence of erythrocytes lowers local oxygen tension, since dissolved O_2 is rapidly bound and consumed, and this reduces the oxygen enhancement effect (OER) of low-LET radiation [23,24]. Furthermore, platelet-rich plasma (PRP), a blood derivative enriched with growth factors and antioxidants, has been shown to reduce UVB-induced apoptosis, decrease pro-inflammatory cytokines, and enhance antioxidant enzyme activities such as superoxide dismutase (SOD) and glutathione peroxidase [25,26]. Collectively, these observations support the contention that blood is not just a reservoir for markers of oxidative stress but is itself an active participant in the protection of the body from UVB damage. This cellular contribution to biochemical buffering likely is responsible for the increased survival and detectability of chromosomal aberrations in whole blood co-exposure models compared to isolated lymphocyte systems. Detection of γH2AX foci in isolated PBMCs and whole blood under all conditions may on a first look seem to be in conflict with the outcome of dicentric assays, which showed evident differences in cell survival and chromosomal aberrations. However, this can be attributed to the distinct biological time windows captured by each method, as γH2AX foci are rapidly formed—within several minutes—at DNA DSBs, and therefore assay is highly sensitive to primary DNA damage. Importantly, γH2AX formation does not require long-term cell survival; even PBMCs that are destined to undergo apoptosis still show foci during the early hours post-irradiation. The similar foci counts observed at 1 h in both systems reflect comparable initial damage induction. In contrast, the dicentric assay requires cells to survive, enter mitosis, and complete at least one division within ~48 hours. As a result, only those lymphocytes that successfully repair or tolerate damage will contribute to dicentric scoring. This explains why isolated PBMCs exposed to 1 Gy gamma rays and 100 J/m² UVB showed early γH2AX foci but failed to survive for chromosomal analysis, whereas whole blood samples, protected by plasma antioxidants and supported by a physiological environment, exhibited robust dicentric yields.

A key observation from our study is the persistence of elevated γH2AX foci at 24 h after UVB exposure. While γH2AX is typically associated with the immediate marking of DSBs, its persistent presence long after irradiation suggests incomplete resolution of DNA damage or ongoing secondary break formation. As previously reported by Freeman et. al [27], UVB irradiation in lymphocytes generates lesions that can persist due to the limited efficiency of nucleotide excision repair (NER) in non-dividing cells. Our finding of elevated γH2AX foci at 24 h may therefore reflect the accumulation of unrepaired or misrepaired lesions, replication-associated conversion of photoproducts into DSBs, or complex DNA Damage formation.

Aside from qualitative observations of increased DNA damage during co-exposure, our statistical analysis using the Bliss Independence Model provides quantitative evidence that gamma and UVB radiation interact synergistically at the cellular level rather than additively, as evidenced by the positive Bliss excess scores in all cases. These findings suggest that gamma and UVB radiation cause DNA damage via independent but complimentary mechanisms, overwhelming repair pathways and amplifying genotoxic effects when stressors are combined leading to increased chromosomal instability and cancer risk.

One of the most serious and well-documented consequences of ionizing radiation exposure is an increased lifetime chance of cancer, which is thought to be the primary stochastic effect. According to the BEIR VII Phase 2 report (National Research Council, 2006), a dosage of 1 Gy from low-LET radiation, such as gamma rays, is related with an estimated 5% increase in lifetime risk for all solid malignancies in an adult population. This estimate is based on epidemiological studies of atomic bomb survivors, medical patients, and occupationally exposed populations, and it employs the linear no-threshold (LNT) model. In this study, we evaluated the cytogenetic impact of single and combined exposures to ionizing (gamma rays) and non-ionizing (UVB) radiation in peripheral blood lymphocytes using the γH2AX immunofluorescence and dicentric chromosome assay. Our results through chromosomal aberration analysis for the 2nd donor demonstrate that while 1 Gy of gamma rays alone produced a mean dicentric frequency of 0.055, the co-exposure condition resulted in a

 doi:10.20944/preprints202509.2609.v1

significantly higher frequency of 0.113 dicentrics per cell. This marked increase suggests a synergistic interaction between the two radiation types, leading to enhanced chromosomal instability.

To interpret the biological significance of this co-exposure, we estimated the equivalent gamma ray dose that would be required to produce the same cytogenetic effect observed under combined exposure conditions. Using a linear-quadratic dose–response model typical of low-LET gamma ray calibration curve produced by Abe et al. [28]: $Y=0.0013+0.0067D+0.0313D^2$ ($r = 0.9985$) we calculated that a dicentric yield of 0.113 corresponds to an effective gamma ray dose of approximately 1.79 Gy, confirming the contribution of UVB in amplifying DNA damage beyond that induced by gamma rays alone.

Importantly, we assessed the potential health implications of such exposures by estimating the associated cancer risk. According to the BEIR VII risk model for low-LET ionizing radiation, each gray of acute exposure increases lifetime cancer risk by approximately 5% [29]. Applying this model to the equivalent dose of 1.79 Gy suggests an excess lifetime cancer risk of around 8.9%. Similarly, for the 1st donor, a dicentric frequency of 0.059 was observed following co-exposure to 1 Gy gamma rays and 100 J/m² UVB. Using the same linear-quadratic dose–response model [28] we estimated that this aberration yield corresponds to an effective gamma ray dose of approximately 1.26 Gy. Applying the BEIR VII cancer risk model, the estimated excess cancer risk for this donor under co-exposure conditions is approximately 6.3%. This value is still higher than the baseline risk associated with 1 Gy exposure alone and further supports the synergistic genotoxic potential of combined gamma and UVB radiation. The lower equivalent dose reflects inter-individual variability in cytogenetic response and reinforces the importance of donor-specific biodosimetry in mixed radiation exposure scenarios. For the 3rd donor, results clearly demonstrate a synergistic genotoxic effect from co-exposure to 1 Gy gamma rays and 100 J/m² UVB, as according to Abe et al.'s linear-quadratic dose-response model, the measured dicentric yield of about 0.112 dicentrics/cell equates to an effective gamma-ray dosage of roughly 1.78 Gy and using the BEIR VII cancer risk model, this dose corresponds to an estimated extra lifetime cancer risk of 8.8%.

The aforementioned findings emphasize the possibility of synergistic interactions between ionizing and non-ionizing radiation amplifying DNA damage and, thus, carcinogenic potential. Beyond cancer, ionizing radiation has been linked to a variety of non-cancer health concerns, particularly when exposure is moderate to high or affects sensitive tissues. Radiation-induced cataracts are a well-documented deterministic consequence, with even modest doses (0.5 Gy) causing opacities in the eye's lens[30]. Cardiovascular effects have also gained significant attention in recent years; studies have shown that radiation doses exceeding 0.5–1.0 Gy to the heart or major arteries are associated with increased risk of ischemic heart disease and stroke [31,32]. Chronic exposure has also been implicated in promoting atherosclerosis and microvascular damage, possibly through persistent inflammation and endothelial dysfunction [33]. Additionally, high-dose radiation to the brain, especially in children, has been linked to neurocognitive impairments and neuroendocrine dysfunctions [34,35].

The use of cytogenetic assays, such as the dicentric chromosome assay, remains a gold standard for estimating absorbed radiation doses and offers insight into potential long-term health effects, including cancer risk [36,37]. The findings of this study reinforce the need to consider combined exposures in radiation protection frameworks, particularly in clinical, occupational, or environmental settings where individuals may be exposed to both ionizing and non-ionizing radiation sources. In addition to increased dicentric chromosome formation, our study revealed a notable presence of acentric fragments in peripheral blood lymphocytes following co-exposure to 1 Gy gamma rays and 100 J/m² UVB. The simultaneous elevation of both aberration types suggests distinct yet complementary damage pathways activated by the combined exposure. The mechanistic differences between dicentrics and fragments become especially relevant in the context of combined gamma rays and UVB exposure [37-39]. Gamma rays induce DSBs via direct ionization and, indirectly, through ROS production, affecting both nuclear and mitochondrial DNA. UVB, although being a non-ionizing radiation, causes bulky DNA lesions such as cyclobCPDs and 6-4 photoproducts, which primarily

 doi:10.20944/preprints202509.2609.v1

stall DNA replication forks and activate the NER pathway [40,41]. When combined, UVB may inhibit accurate DSB repair by either saturating repair machinery or interfering with signaling cascades such as ATM/ATR and p53. This replication stress can convert UVB-induced lesions into DSBs during the S-phase, further compounding the damage initiated by gamma rays. The net result is both increased misrejoining (yielding dicentrics) and accumulated unrepaired breaks (leading to fragments) [42]. Biologically, the presence of both dicentrics and fragments indicates not only enhanced chromosomal instability but also increased cell heterogeneity, which is a known cause of clonal evolution and cancer[43]. While dicentrics are unstable and often removed during cell division, acentric fragments can persist longer and may be incorporated into micronuclei, contributing to chromothripsis-like events and long-term genomic instability [7,44,45].

5. Conclusions

Exposing PBMCs to both gamma rays and UVB radiation causes a synergistic increase in DNA damage, as shown by increased dicentric formation and γH2AX signaling. To forecast dicentric yields, an enhanced linear-quadratic model was devised, which included interaction terms that were dependent on dosage time and radiation sequence. The model correctly captured observed patterns across several donors and sample types, demonstrating its usefulness in mixed-radiation biodosimetry. These findings emphasize the significance of exposure context and encourage the use of synergy-based modeling in future radiation risk evaluations.

Supplementary Materials: The following supporting information can be downloaded at the website of this paper posted on Preprints.org. Table S2.1: Values of erythemal weighted irradiances Eff (W/m²) in different heights.; title; Table S2.2: Values of absolute irradiances based on the spectral conversion factor given by the manufacturer; Figure S2: Irradiation setups.; Figure S3: Dose effect curve in PBMCs of the 1st donor.

Author Contributions: Conceptualization, A.G.G.; methodology, A.G.G., A.G. and G.I.T.; software, A.G., A.A., D.D., S.T., P.M., S.V. and G.T.; formal analysis, A.G., A.A.; investigation, A.G., A.A. and G.M.; data curation, A.G. A.A., D.D. and A.G.G.; writing—original draft preparation, A.G., A.A., S.T., G.M. and G.I.T; writing—review and editing, all authors; supervision, A.G.G.; project administration, A.G.G.; funding acquisition, A.G.G. All authors have read and agreed to the published version of the manuscript.

Funding: All authors acknowledge funding from project BIOSPHERE (No. 21GRD02) that has received funding from the European Partnership on Metrology, co-financed by the European Union's Horizon Europe Research and Innovation Programme and by the Participating States.

Institutional Review Board Statement: The study was conducted in accordance with the Declaration of Greece, and approved by the NCSR 'Demokritos' bioethics committee (21/12/2023-17 (Date: 21/02/2023)).

Informed Consent Statement: Written informed consent has been obtained from the patients to publish this paper.

Acknowledgments: We gratefully acknowledge Faton Krasniqi (PTB) for his leadership of the project BIOSPHERE (No. 21GRD02) and for his valuable guidance throughout this work. We would like to thank Aspasia Petri (GAEC) for providing the UV radiometer and calibrating the UVB radiation source.

Conflicts of Interest: The authors declare no conflicts of interest.

References

1. Volatier, T.; Schumacher, B.; Meshko, B.; Hadrian, K.; Cursiefen, C.; Notara, M. Short-Term UVB Irradiation Leads to Persistent DNA Damage in Limbal Epithelial Stem Cells, Partially Reversed by DNA Repairing Enzymes. *Biology* **2023**, *12*, 265.
2. Rastogi, R.P.; Richa; Kumar, A.; Tyagi, M.B.; Sinha, R.P. Molecular Mechanisms of Ultraviolet Radiation-Induced DNA Damage and Repair. *Journal of Nucleic Acids* **2010**, *2010*, 592980, doi:https://doi.org/10.4061/2010/592980.
3. Nickoloff, J.A.; Sharma, N.; Taylor, L. Clustered DNA Double-Strand Breaks: Biological Effects and Relevance to Cancer Radiotherapy. *Genes (Basel)* **2020**, *11*, doi:10.3390/genes11010099.

 doi:10.20944/preprints202509.2609.v1

4. Mladenova, V.; Mladenov, E.; Stuschke, M.; Iliakis, G. DNA Damage Clustering after Ionizing Radiation and Consequences in the Processing of Chromatin Breaks. *Molecules* **2022**, *27*, 1540.
5. Mavragani, I.V.; Nikitaki, Z.; Kalospyros, S.A.; Georgakilas, A.G. Ionizing Radiation and Complex DNA Damage: From Prediction to Detection Challenges and Biological Significance. *Cancers* **2019**, *11*, 1789.
6. Gkikoudi, A.; Manda, G.; Beinke, C.; Giesen, U.; Al-Qaaod, A.; Dragnea, E.-M.; Dobre, M.; Neagoe, I.V.; Sangsuwan, T.; Haghdoost, S.; et al. Synergistic Effects of UVB and Ionizing Radiation on Human Non-Malignant Cells: Implications for Ozone Depletion and Secondary Cosmic Radiation Exposure. *Biomolecules* **2025**, *15*, 536.
7. Pantelias, A.; Karachristou, I.; Georgakilas, A.G.; Terzoudi, G.I. Interphase Cytogenetic Analysis of Micronucleated and Multinucleated Cells Supports the Premature Chromosome Condensation Hypothesis as the Mechanistic Origin of Chromothripsis. *Cancers (Basel)* **2019**, *11*, doi:10.3390/cancers11081123.
8. Tremi, I.; Havaki, S.; Georgitsopoulou, S.; Terzoudi, G.; Lykakis, I.N.; Iliakis, G.; Georgakilas, V.; Gorgoulis, V.G.; Georgakilas, A.G. Biological Response of Human Cancer Cells to Ionizing Radiation in Combination with Gold Nanoparticles. *Cancers* **2022**, *14*, 5086.
9. Nikitaki, Z.; Pariset, E.; Sudar, D.; Costes, S.V.; Georgakilas, A.G. In Situ Detection of Complex DNA Damage Using Microscopy: A Rough Road Ahead. *Cancers* **2020**, *12*, 3288.
10. Wu, S.; Li, X.; Gao, F.; de Groot, J.F.; Koul, D.; Yung, W.K.A. PARP-mediated PARylation of MGMT is critical to promote repair of temozolomide-induced O6-methylguanine DNA damage in glioblastoma. *Neuro-Oncology* **2021**, *23*, 920-931, doi:10.1093/neuonc/noab003.
11. Zhao, W.; Sachsenmeier, K.; Zhang, L.; Sult, E.; Hollingsworth, R.E.; Yang, H. A New Bliss Independence Model to Analyze Drug Combination Data. *SLAS Discovery* **2014**, *19*, 817-821, doi:10.1177/1087057114521867.
12. McMahon, S.J. The linear quadratic model: usage, interpretation and challenges. *Phys Med Biol* **2018**, *64*, 01tr01, doi:10.1088/1361-6560/aaf26a.
13. Holmberg, M.; Strausmanis, R. The repair of chromosome aberrations in human lymphocytes after combined irradiation with UV-radiation (254 nm) and X-rays. *Mutat Res* **1983**, *120*, 45-50, doi:10.1016/0165-7992(83)90072-6.
14. Aranda-Rivera, A.K.; Cruz-Gregorio, A.; Arancibia-Hernández, Y.L.; Hernández-Cruz, E.Y.; Pedraza-Chaverri, J. RONS and Oxidative Stress: An Overview of Basic Concepts. *Oxygen* **2022**, *2*, 437-478.
15. Altomare, A.; Baron, G.; Brioschi, M.; Longoni, M.; Butti, R.; Valvassori, E.; Tremoli, E.; Carini, M.; Agostoni, P.; Vistoli, G.; et al. N-Acetyl-Cysteine Regenerates Albumin Cys34 by a Thiol-Disulfide Breaking Mechanism: An Explanation of Its Extracellular Antioxidant Activity. *Antioxidants* **2020**, *9*, 367.
16. Grigoryan, H.; Li, H.; Iavarone, A.T.; Williams, E.R.; Rappaport, S.M. Cys34 adducts of reactive oxygen species in human serum albumin. *Chem Res Toxicol* **2012**, *25*, 1633-1642, doi:10.1021/tx300096a.
17. Roche, M.; Rondeau, P.; Singh, N.R.; Tarnus, E.; Bourdon, E. The antioxidant properties of serum albumin. *FEBS Letters* **2008**, *582*, 1783-1787, doi:https://doi.org/10.1016/j.febslet.2008.04.057.
18. Glantzounis, G.K.; Tsimoyiannis, E.C.; Kappas, A.M.; Galaris, D.A. Uric acid and oxidative stress. *Curr Pharm Des* **2005**, *11*, 4145-4151, doi:10.2174/138161205774913255.
19. de Oliveira, E.P.; Burini, R.C. High plasma uric acid concentration: causes and consequences. *Diabetol Metab Syndr* **2012**, *4*, 12, doi:10.1186/1758-5996-4-12.
20. Sautin, Y.Y.; Johnson, R.J. Uric acid: the oxidant-antioxidant paradox. *Nucleosides Nucleotides Nucleic Acids* **2008**, *27*, 608-619, doi:10.1080/15257770802138558.
21. Daraghmeh, D.N.; Karaman, R. The Redox Process in Red Blood Cells: Balancing Oxidants and Antioxidants. *Antioxidants* **2025**, *14*, 36.
22. Kuhn, V.; Diederich, L.; Keller, T.C.S.t.; Kramer, C.M.; Lückstädt, W.; Panknin, C.; Suvorava, T.; Isakson, B.E.; Kelm, M.; Cortese-Krott, M.M. Red Blood Cell Function and Dysfunction: Redox Regulation, Nitric Oxide Metabolism, Anemia. *Antioxid Redox Signal* **2017**, *26*, 718-742, doi:10.1089/ars.2016.6954.
23. Gray, L.H.; Conger, A.D.; Ebert, M.; Hornsey, S.; Scott, O.C. The concentration of oxygen dissolved in tissues at the time of irradiation as a factor in radiotherapy. *Br J Radiol* **1953**, *26*, 638-648, doi:10.1259/0007-1285-26-312-638.

 doi:10.20944/preprints202509.2609.v1

24. Grimes, D.R.; Partridge, M. A mechanistic investigation of the oxygen fixation hypothesis and oxygen enhancement ratio. *Biomed Phys Eng Express* **2015**, *1*, 045209, doi:10.1088/2057-1976/1/4/045209.
25. Duan, G.H.; Ren, Z.Q.; Du, B.; Shao, W.; Dong, H.J.; Du, A.C. Platelet-rich plasma protects human keratinocytes from UVB-induced apoptosis by attenuating inflammatory responses and endoplasmic reticulum stress. *J Cosmet Dermatol* **2023**, *22*, 1327-1333, doi:10.1111/jocd.15559.
26. Cui, X.; Ma, Y.; Wang, H.; Huang, J.; Li, L.; Tang, J.; Cheng, B. The Anti-photoaging Effects of Pre- and Post-treatment of Platelet-rich Plasma on UVB-damaged HaCaT Keratinocytes. *Photochem Photobiol* **2021**, *97*, 589-599, doi:10.1111/php.13354.
27. Freeman, S.E.; Applegate, L.A.; Ley, R.D. EXCISION REPAIR OF UVR-INDUCED PYRIMIDINE DIMERS IN CORNEAL DNA. *Photochemistry and Photobiology* **1988**, *47*, 159-163, doi:https://doi.org/10.1111/j.1751-1097.1988.tb02707.x.
28. Abe, Y.; Yoshida, M.A.; Fujioka, K.; Kurosu, Y.; Ujiie, R.; Yanagi, A.; Tsuyama, N.; Miura, T.; Inaba, T.; Kamiya, K.; et al. Dose–response curves for analyzing of dicentric chromosomes and chromosome translocations following doses of 1000 mGy or less, based on irradiated peripheral blood samples from five healthy individuals. *Journal of Radiation Research* **2017**, *59*, 35-42, doi:10.1093/jrr/rrx052.
29. Council, N.R. *Health Risks from Exposure to Low Levels of Ionizing Radiation: BEIR VII Phase 2*; The National Academies Press: Washington, DC, 2006; p. 422.
30. Stewart, F.A.; Akleyev, A.V.; Hauer-Jensen, M.; Hendry, J.H.; Kleiman, N.J.; Macvittie, T.J.; Aleman, B.M.; Edgar, A.B.; Mabuchi, K.; Muirhead, C.R.; et al. ICRP publication 118: ICRP statement on tissue reactions and early and late effects of radiation in normal tissues and organs--threshold doses for tissue reactions in a radiation protection context. *Ann ICRP* **2012**, *41*, 1-322, doi:10.1016/j.icrp.2012.02.001.
31. Little, M.P.; Azizova, T.V.; Richardson, D.B.; Tapio, S.; Bernier, M.O.; Kreuzer, M.; Cucinotta, F.A.; Bazyka, D.; Chumak, V.; Ivanov, V.K.; et al. Ionising radiation and cardiovascular disease: systematic review and meta-analysis. *Bmj* **2023**, *380*, e072924, doi:10.1136/bmj-2022-072924.
32. Kreuzer, M.; Auvinen, A.; Cardis, E.; Hall, J.; Jourdain, J.-R.; Laurier, D.; Little, M.P.; Peters, A.; Raj, K.; Russell, N.S.; et al. Low-dose ionising radiation and cardiovascular diseases – Strategies for molecular epidemiological studies in Europe. *Mutation Research/Reviews in Mutation Research* **2015**, *764*, 90-100, doi:https://doi.org/10.1016/j.mrrev.2015.03.002.
33. Baselet, B.; Rombouts, C.; Benotmane, A.M.; Baatout, S.; Aerts, A. Cardiovascular diseases related to ionizing radiation: The risk of low-dose exposure (Review). *Int J Mol Med* **2016**, *38*, 1623-1641, doi:10.3892/ijmm.2016.2777.
34. Mulhern, R.K.; Merchant, T.E.; Gajjar, A.; Reddick, W.E.; Kun, L.E. Late neurocognitive sequelae in survivors of brain tumours in childhood. *Lancet Oncol* **2004**, *5*, 399-408, doi:10.1016/s1470-2045(04)01507-4.
35. Greene-Schloesser, D.; Robbins, M.E. Radiation-induced cognitive impairment--from bench to bedside. *Neuro Oncol* **2012**, *14 Suppl 4*, iv37-44, doi:10.1093/neuonc/nos196.
36. *Cytogenetic Dosimetry: Applications in Preparedness for and Response to Radiation Emergencies*; INTERNATIONAL ATOMIC ENERGY AGENCY: Vienna, 2011.
37. Fenech, M.; Kirsch-Volders, M.; Natarajan, A.T.; Surralles, J.; Crott, J.W.; Parry, J.; Norppa, H.; Eastmond, D.A.; Tucker, J.D.; Thomas, P. Molecular mechanisms of micronucleus, nucleoplasmic bridge and nuclear bud formation in mammalian and human cells. *Mutagenesis* **2011**, *26*, 125-132, doi:10.1093/mutage/geq052.
38. Mazzagatti, A.; Engel, J.L.; Ly, P. Boveri and beyond: Chromothripsis and genomic instability from mitotic errors. *Molecular Cell* **2024**, *84*, 55-69, doi:https://doi.org/10.1016/j.molcel.2023.11.002.
39. Levine, M.S.; Holland, A.J. The impact of mitotic errors on cell proliferation and tumorigenesis. *Genes Dev* **2018**, *32*, 620-638, doi:10.1101/gad.314351.118.
40. Cadet, J.; Sage, E.; Douki, T. Ultraviolet radiation-mediated damage to cellular DNA. *Mutat Res* **2005**, *571*, 3-17, doi:10.1016/j.mrfmmm.2004.09.012.
41. Daya-Grosjean, L.; Sarasin, A. The role of UV induced lesions in skin carcinogenesis: an overview of oncogene and tumor suppressor gene modifications in xeroderma pigmentosum skin tumors. *Mutat Res* **2005**, *571*, 43-56, doi:10.1016/j.mrfmmm.2004.11.013.
42. Pfeiffer, P.; Goedecke, W.; Obe, G. Mechanisms of DNA double-strand break repair and their potential to induce chromosomal aberrations. *Mutagenesis* **2000**, *15*, 289-302, doi:10.1093/mutage/15.4.289.

 doi:10.20944/preprints202509.2609.v1

43. Burrell, R.A.; McGranahan, N.; Bartek, J.; Swanton, C. The causes and consequences of genetic heterogeneity in cancer evolution. *Nature* **2013**, *501*, 338-345, doi:10.1038/nature12625.
44. Krupina, K.; Goginashvili, A.; Cleveland, D.W. Causes and consequences of micronuclei. *Curr Opin Cell Biol* **2021**, *70*, 91-99, doi:10.1016/j.ceb.2021.01.004.
45. Zhang, C.Z.; Spektor, A.; Cornils, H.; Francis, J.M.; Jackson, E.K.; Liu, S.; Meyerson, M.; Pellman, D. Chromothripsis from DNA damage in micronuclei. *Nature* **2015**, *522*, 179-184, doi:10.1038/nature14493.